Construction of Protein-Based Biosensors Using Ligand-Directed Chemistry for Detecting Analyte Binding

Kei Yamaura*, Shigeki Kiyonaka*, Itaru Hamachi*,†,1
*Graduate School of Engineering, Kyoto University, Katsura, Kyoto, Japan
†Core Research for Evolutional Science and Technology (CREST), Japan Science and Technology Agency, Kawaguchi, Saitama, Japan
[1]Corresponding author: e-mail address: ihamachi@sbchem.kyoto-u.ac.jp

Contents

Abstract

Protein-based fluorescent biosensors are powerful tools for quantitative detection of biomolecules or drugs with high sensitivity under physiological conditions. However,

Methods in Enzymology
ISSN 0076-6879
http://dx.doi.org/10.1016/bs.mie.2017.02.006

conventional methods for construction of biosensors require structural data with high resolution or amino acid sequence information in most cases, which hampers applicability of this method to structurally complicated receptor proteins. To sidestep such limitations, we recently developed a new method that employs ligand-directed chemistry coupled with a bimolecular fluorescence quenching and recovery system, which enabled the conversion of various kinds of membrane-bound receptors to "turn-on" type fluorescent sensors. Here, we describe a protocol for construction of "turn-on" type fluorescent biosensors based on the $GABA_A$ receptor which permits quantitative analysis of the ligand affinity.

1. INTRODUCTION

Currently, drug discovery programs are largely dependent on screening large libraries of small chemicals for their effects on target proteins, and new strategies are required for rapid and efficient screening (Loving, Sainlos, & Imperiali, 2010; Mayr & Bojanic, 2009; Prével, Pellerano, Van, & Morris, 2014). One of the potential methods relies on a protein-based fluorescent biosensor, which permits quantitative detection of biomolecules or drugs with high sensitivity in the physiological environment. In most cases, these biosensors detect ligands by transducing the large structural changes upon ligand binding as changes in fluorescence (Tamura & Hamachi, 2014). These are constructed by conjugation of fluorescent proteins with a ligand-binding domain (LBD) (Fehr, Frommer, & Lalonde, 2002; Marvin et al., 2013; Okumoto et al., 2005) or by site-directed modification of an introduced cysteine residue near the ligand-binding site with a small fluorophore (Marvin & Hellinga, 1998; Morii et al., 2002; Simard, Getlik, et al., 2009; Simard, Klüter, et al., 2009; Takikawa et al., 2014).

Recently, a new technique which does not require protein structural changes upon ligand binding has been reported for construction of biosensors (Brun et al., 2012; Brun, Tan, Nakata, Hinner, & Johnsson, 2009; Masharina, Reymond, Maurel, Umezawa, & Johnsson, 2012). These biosensors, termed Snifts (SNAP-tag-based indicator proteins with a fluorescent intramolecular tether), consist of SNAP-tag, CLIP-tag, and LBD, where SNAP-tag is labeled with a small molecular tether bearing a ligand to the LBD and a fluorescent acceptor, and the CLIP-tag is modified with a fluorescent donor. In this method, the covalently attached ligand is displaced from the binding site of the LBD by addition of competitive compounds,

resulting in a change in the relative position of the acceptor and the donor, so that the fluorescent signal can be modulated upon the competitor's binding without any need for structural changes in the LBD. While these protein-based biosensors mentioned earlier are very powerful, most of them require structural information on the target protein and strongly rely on genetic manipulation.

We recently reported ligand-directed chemistry for selective labeling of target proteins, in which neither structural information on the LBD nor genetic manipulation are required (Fig. 1) (Fujishima, Yasui, Miki, Ojida, & Hamachi, 2012; Takaoka, Nishikawa, Hashimoto, Sasaki, & Hamachi, 2015; Tsukiji, Miyagawa, Takaoka, Tamura, & Hamachi, 2009). Covalent labeling of proteins using ligand-directed chemistry is driven by selective ligand–protein recognition, which facilitates a chemical reaction of a reactive group having moderate reactivity with nucleophilic amino acid residues located near the LBD with the help of the proximity effect. Importantly, the protein function can be recovered by washing out the excess labeling reagents and the remaining ligand moieties even after the chemical modification. Using ligand-directed acyl imidazole (LDAI) chemistry which is powerful for membrane-protein labeling, we succeeded in chemical labeling of folate receptors on live cells (Fujishima et al., 2012). To our surprise, a fluorescence increase occurred upon addition of ligands such as folic acid and its derivatives, implying that the labeled folate receptors

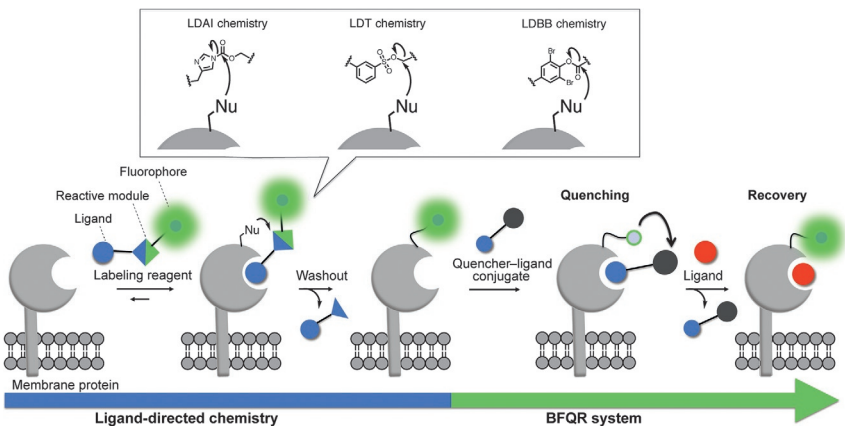

Fig. 1 Construction of protein-based fluorescent biosensors by coupling affinity-based chemical labeling (*left*) with BFQR system (*right*). Schematic illustration for fluorescent labeling using ligand-directed chemistry and the construction of fluorescent biosensors using BFQR system are shown. *Nu*: nucleophile.

can be converted to a fluorescence biosensor. A recent crystal structural analysis reveals there are a few tryptophan residues near the LBD (Chen et al., 2013), which indicates that this fluorescence change would likely be caused by relief of the tryptophan-induced quenching of the labeled fluorophore upon ligand binding. However, such an ideal arrangement of tryptophan residues does not always occur in every LBD of target protein scaffolds, which raises a serious limitation in the applicability of this technology to a wider variety of receptor proteins.

To overcome this limitation, we also developed a method using chemical labeling coupled with bimolecular fluorescence quenching and recovery (BFQR) system. This approach is expected to be more general for constructing fluorescent biosensors since the protein need not provide the quenching species (Fig. 1) (Wang et al., 2011). In this method, after the covalent attachment of a fluorophore in the vicinity of the ligand-binding site, the fluorescence is efficiently quenched by the quencher–ligand conjugate. When the conjugate bound to the ligand-binding site is competitively replaced with small molecules having a sufficient affinity for the same binding site, efficient recovery of the fluorescence (that is, in the turn-on mode) takes place. This method was initially applied to bradykinin receptor 2 and is now extended to various kinds of membrane-surface receptors.

$GABA_A$ receptors ($GABA_ARs$) have been widely recognized as an important drug target over many years (Barnard et al., 1998; Chebib & Johnston, 2000), and a wide variety of orthosteric ligands and allosteric modulators have been reported for $GABA_ARs$ (Fig. 2). Among them,

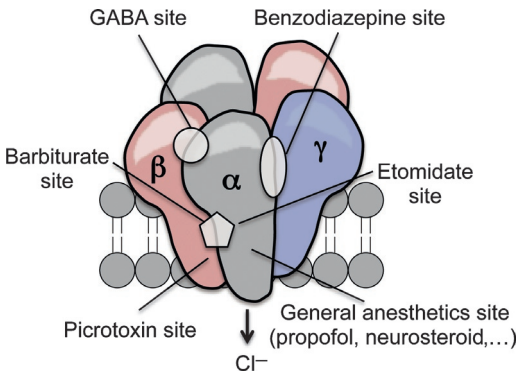

Fig. 2 Structural illustration of $GABA_ARs$ and associated ligand-binding sites. *Reproduced from Yamaura, K., Kiyonaka, S., Numata, T., Inoue, R., & Hamachi, I. (2016). Discovery of allosteric modulators for $GABA_A$ receptors by ligand-directed chemistry.* Nature Chemical Biology, 12, *822–830, with permission from Nature Publishing Group.*

benzodiazepine derivatives exhibit potent sedative/hypnotic and anxiolytic effects (Rudolph & Knoflach, 2011). Barbiturates, etomidate, propofol, and neurosteroids, whose binding sites are located elsewhere on the molecule from that of benzodiazepines, are widely utilized as anesthetics (Sieghart, 2015). Recently, we developed "turn-on" fluorescent biosensors for $GABA_AR$ ligands using LDAI chemistry coupled with the BFQR system (Fig. 1) (Yamaura, Kiyonaka, Numata, Inoue, & Hamachi, 2016). To date, two fluorescent sensors based on $GABA_ARs$ which can respond to orthosteric GABA-site ligands or allosteric benzodiazepine-site ligands have been developed. Here, we provide a step-by-step protocol for researchers who are interested in construction of BFQR-based fluorescent biosensors.

2. EXPRESSION OF $GABA_AR$ CONSISTING OF α/β/γ SUBUNITS IN HEK293T CELLS

$GABA_ARs$ assemble into a heteropentamer consisting of a variety of subunits to form GABA-gated chloride channels. To date, 19 different subunits (α1–α6, β1–β3, γ1–γ3, δ, ε, π, θ, and ρ1–ρ3) have been identified in $GABA_ARs$, which gives rise to a remarkable level of diversity and complexity. Recent studies have demonstrated that physiologically relevant heteromeric $GABA_AR$ forms are mainly composed of two α subunits, two β subunits, and one γ subunit, and that at least 20–30 isoforms consisting of different combinations of these subunits are expressed in the brain (Olsen & Sieghart, 2009). In pharmacological assays using neuronal samples, complicated responses to each drug are observed because each $GABA_AR$ exhibits distinct pharmacological properties. In contrast, a single isoform of $GABA_AR$ consisting of α/β/γ subunits can be expressed in human embryonic kidney (HEK) 293T cells, a mammalian cell line, using a conventional transfection method. Importantly, electrophysiological assays revealed that this expression system gives a functional $GABA_AR$-pentamer consisting of α/β/γ subunits in a 2:2:1 ratio (Tretter, Ehya, Fuchs, & Sieghart, 1997; Yamaura et al., 2016). Here, our protocols for recombinant expression of α/β/γ $GABA_ARs$ in HEK293T cells are described later in detail.

1. Culture HEK293T cells in Dulbecco's modified Eagle's medium (DMEM) containing 10% fetal bovine serum, 30 units mL^{-1} penicillin, and 30 units mL^{-1} streptomycin under 95% air-5% CO_2 atmosphere at 37°C.
2. One day before transfection, seed the cells (2.0×10^5 cells) on 3.5-cm primaria dishes (BD Falcon).

3. Mix 0.7 μg of each expression vector for α, β, and γ subunit (total 2.1 μg) and 0.3 μg of pmCherry-N1 (Clontech) as a transfection marker in a microcentrifuge tube and dilute with 50 μL of Opti-MEM.
4. Dilute 2 μL of Lipofectamine 2000 (Invitrogen) with 50 μL of Opti-MEM in a different tube and incubate for 5 min at room temperature.
5. Mix the plasmid solution with the Lipofectamine solution by pipetting several times and incubate for 20 min at room temperature.
6. Directly add the mixed solution into culture dishes.
7. After 4 h incubation, replace the culture medium with fresh medium.
8. After 42–54 h incubation at 37°C with 5% CO_2, utilize the cells for labeling experiments.

3. DESIGN AND SYNTHESIS OF LABELING REAGENTS FOR $GABA_AR$

In recent years, we have succeeded in chemical labeling of various membrane proteins including carbonic anhydrase 12, folate receptor, bradykinin receptor, NMDA receptor, and $GABA_AR$ on live cell surfaces using LDAI chemistry (Fig. 3A, Fujishima et al., 2012; Miki et al., 2014; Yamaura et al., 2016). For selective labeling to a target protein, careful molecular design of LDAI reagents is essential. In this section, we describe the design strategy of LDAI reagents for $GABA_AR$ and the synthetic procedure later.

3.1 Design of LDAI Reagents for $GABA_AR$

LDAI reagents consist of four modules: (a) an acyl imidazole moiety as the cleavable reactive group, (b) a ligand moiety having sufficient affinity and selectivity for the target protein, (c) a spacer moiety between acyl imidazole and the ligand, and (d) a fluorophore (or probe) group. For chemical labeling to $GABA_AR$, we prepared three LDAI reagents (**GGAM-Gaba**, **GGAM-Bzp**, or **GGAM-Bbr**), which are targeted for the orthosteric GABA-, allosteric benzodiazepine-, or barbiturate-site, respectively (Fig. 3B and C). As a typical example, we here describe how to design a LDAI reagent for benzodiazepine site (**CGAM-Bzp**) in detail.

1. Appropriate selection of the ligand moiety is critical in LDAI chemistry. A ligand highly selective for the target protein should be chosen. Employing low-affinity ligands would likely cause nonspecific labeling due to the presence of high concentrations of unbound LDAI reagents. So far, we have obtained successful results using highly specific ligands

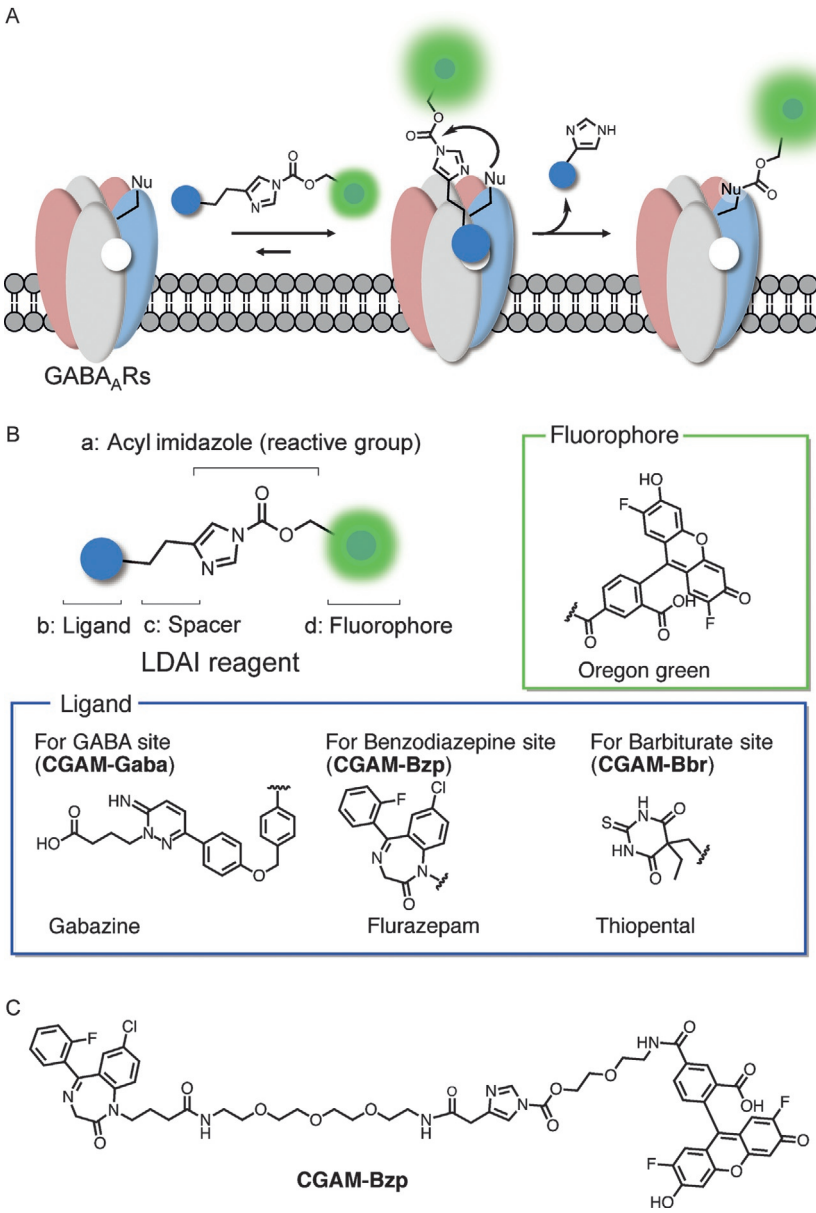

Fig. 3 Chemical labeling and molecular design of GABA$_A$R by LDAI chemistry. (A) Schematic illustration of fluorescent labeling for GABA$_A$R using LDAI chemistry. *Nu*: nucleophile. (B) Basic design configuration of LDAI reagents for GABA$_A$Rs. (C) Chemical structure of LDAI reagent (CGAM-Bzp) for benzodiazepine-site labeling.

with dissociation constants (K_d values) below μ*M* (Fujishima et al., 2012; Miki et al., 2014; Yamaura et al., 2016). It should also be noted that use of a ligand with too high an affinity may perturb the receptor function due to the difficulty of removing the cleaved ligand fragment from the ligand-binding pocket of the target protein after labeling. For labeling the benzodiazepine site, we selected a flurazepam derivative as the ligand moiety for the LDAI reagent (Fig. 3B). This moiety is well known as a highly selective ligand for the benzodiazepine site, showing K_i values of 170 n*M* for $GABA_AR$ (Hanson & Czajkowski, 2008).

2. The acyl imidazole group of LDAI reagents acts as a moderately reactive electrophile. It was demonstrated that positioning this group on the protein surface close to the ligand-binding site facilitates acyl substitution reaction with nucleophilic amino acid residues (Lys, Ser, Thr, or Tyr) (Matsuo et al., 2013; Miki et al., 2016). In other words, the labeling efficiency is largely governed by the proximity between the reactive group of the LDAI reagent and these amino acid side chains on the target protein. Thus, optimization of the spacer length between ligand moiety and the reactive group is crucial for optimizing the labeling efficiency at a high level. Actually, in the case of LDAI labeling at the benzodiazepine site, we found that the labeling yield was dependent on the spacer length (unpublished results), and one of the optimal spacers was triethylene glycol as shown in Fig. 3C.
3. For chemical labeling of surface-exposed membrane proteins such as $GABA_ARs$ on live cells, LDAI reagents should be hydrophilic or negatively charged, which suppresses unfavorable permeation of the LDAI reagents into the live cells. If LDAI reagents permeate into the intracellular region, it would result in nonspecific labeling and high background fluorescence in intracellular spaces. Here, we chose Oregon Green™ (OG) which has a negative charge as the fluorophore group. Compared with fluorescein, OG shows higher photostability and less pH sensitivity.

3.2 Synthesis of LDAI Reagent for $GABA_AR$

Procedures for chemical synthesis of **CGAM-Bzp** (compound 4 in Fig. 4) are described in detail later (Fig. 4).

Synthesis of compound 3

1. Prepare a round-bottom flask containing compound **1** (Yamaura et al., 2016) (18 mg, 0.027 mmol) in anhydrous DMF (270 μL) under N_2 atmosphere.

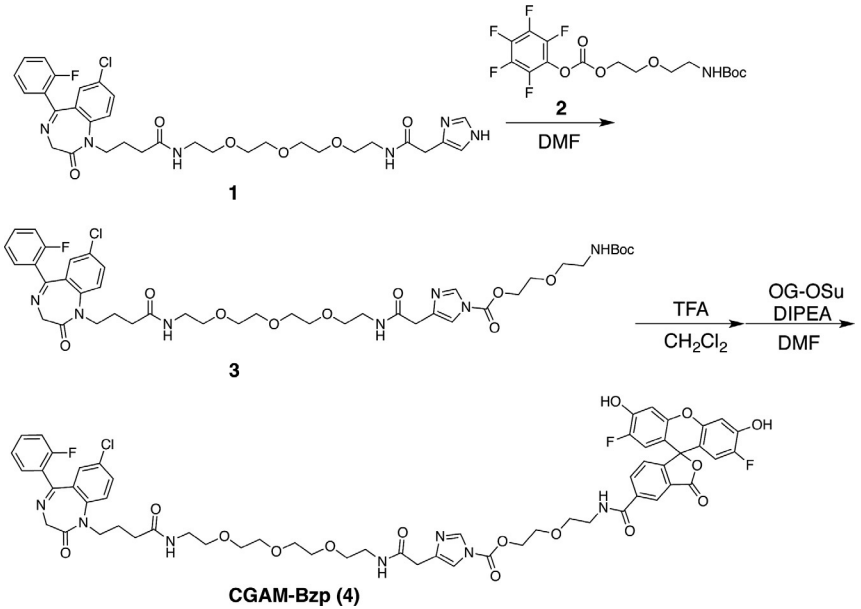

Fig. 4 Synthesis of CGAM-Bzp. *Reproduced from Yamaura, K., Kiyonaka, S., Numata, T., Inoue, R., & Hamachi, I. (2016). Discovery of allosteric modulators for $GABA_A$ receptors by ligand-directed chemistry.* Nature Chemical Biology, 12, *822–830, with permission from Nature Publishing Group.*

2. Add compound **2** (Yamaura et al., 2016) (17 mg, 0.04 mmol).
3. Stir the reaction mixture for 1 h at room temperature.
4. Purify the mixture by silica gel column chromatography ($CHCl_3$ only → $CHCl_3$:MeOH = 10:1) to obtain compound **3** (15 mg, 0.017 mmol, 63%) as a clear solid.
5. *Caution*: compound **3** should be kept in freezer or deep-freezer to prevent decomposition.

Synthesis of CGAM-Bzp (4)

1. Prepare a round-bottom flask containing compound **3** (1.0 mg, 1.1 μmol) in dry CH_2Cl_2 (0.5 mL) under N_2 atmosphere.
2. Add TFA (0.5 mL).
3. Stir the reaction mixture for 1 h at room temperature.
4. Add toluene for azeotropic removal of TFA by rotary evaporation under vacuum. Repeat this step again.
5. Dissolve the residue in dry DMF (100 μL).

6. Add Oregon Green® 488 Carboxylic Acid, Succinimidyl Ester, 5-isomer (Thermo-Fisher, 1 mg, 2.0 μmol), and DIPEA (20 μL, 0.11 mmol).
7. Stir the reaction mixture for 1 h at room temperature.
8. Dilute the reaction mixture with DMSO.
9. Directly purify the mixture by HPLC (mobile phase; CH_3CN (solvent A), 10 m*M* $AcONH_4$ aq. (solvent B)). After purification, go to the next step immediately.
10. Freeze dry the collected fraction to obtain **CGAM-Bzp** (0.8 mg, 0.7 μmol, 64%) as a yellow solid.
11. Dissolve a portion of **CGAM-Bzp** in DMSO to make a stock solution, and determine the **CGAM-Bzp** concentration by UV–vis measurement ($\varepsilon_{495\,nm} = 76{,}000\ M^{-1}\ cm^{-1}$).
12. *Caution*: **CGAM-Bzp** or its DMSO solution should be kept in the deep-freezer to prevent the decomposition.

Caution in the synthesis: The acyl imidazole group is not stable under acidic or basic aqueous conditions. Therefore, compound **3** and **CGAM-Bzp** should be carefully purified by silica gel column chromatography or HPLC under neutral conditions (Miki et al., 2014; Yamaura et al., 2016).

4. CHEMICAL LABELING OF $GABA_AR$ USING LDAI REAGENT

Chemical labeling protocols for $GABA_AR$ on live cells are described in this section. For confirmation of covalent labeling to target proteins, we generally utilize analytical methods including Western blotting and confocal laser scanning microscopy (CLSM) imaging. In addition, the labeled amino acid residues with LDAI reagents are determined by peptide mass fingerprinting analysis.

4.1 Confirmation of Chemical Labeling of $GABA_AR$ by CLSM

CLSM analyses provide valuable information on chemical labeling by LDAI reagents. In addition to chemical labeling of surface-exposed $GABA_AR$, the impermeability of the LDAI reagent, which is also essential for selective visualization of surface-exposed receptors, can be evaluated by CLSM. Although the CLSM observation is performed after washing several times to remove excess LDAI reagent, we cannot exclude the possibility that the observed fluorescence comes from the LDAI reagent noncovalently bound to target proteins. In most cases, however, we confirm that the

washing procedure suffices to remove the unreacted labeling reagent and any remaining ligand moiety from target proteins when the ligand moiety has moderate affinity as described in Section 3.1.

To confirm selective labeling of $GABA_AR$, we perform negative control experiments (Fig. 5). While CLSM imaging visualized prominent fluorescence from surface of the cell transfected with α1/β3/γ2 $GABA_ARs$ after treatment with the LDAI reagents, the fluorescence was observed neither in empty vector-transfected cells nor in α1/β3/γ2 $GABA_AR$-transfected cells pretreated with competitive inhibitors. These negative control experiments verify the specific labeling to $GABA_AR$.

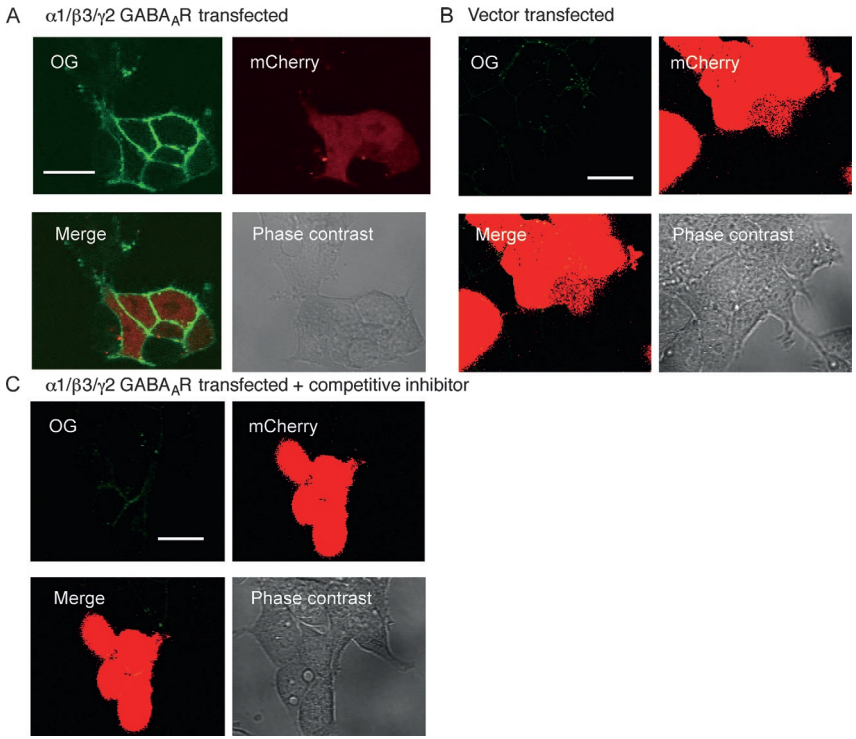

Fig. 5 CLSM imaging visualizes chemical labeling of $GABA_ARs$ using CGAM(Bzp). (A–C) HEK293T cells transfected with α1/β3/γ2 $GABA_ARs$ in (A or C) or control vector in (B) were incubated with 2 μ*M* CGAM-Bzp in serum-free DMEM at 37°C for 3 h in the absence (A or B) or presence of 20 μ*M* flumazenil (competitive inhibitor) in (C). mCherry-N1 was utilized as a transfection marker. Scale bars: 20 μm. *Reproduced from Yamaura, K., Kiyonaka, S., Numata, T., Inoue, R., & Hamachi, I. (2016). Discovery of allosteric modulators for $GABA_A$ receptors by ligand-directed chemistry.* Nature Chemical Biology, 12, *822–830, with permission from Nature Publishing Group.*

The protocols for CLSM imaging of $GABA_AR$ using **CGAM-Bzp** were described later. In a similar manner, we succeeded in selective labeling of $GABA_AR$ using **CGAM-Gaba** by similar procedures.

1. After 24 h of transfection, dissociate transfected cells by pipetting and reseed on glass-bottom dishes (Iwaki) pretreated with poly-L-lysine.
2. 18–30 h after the reseeding, replace the culture medium with serum-free-DMEM medium containing 2 μ*M* **CGAM-Bzp**. *Caution*: **CGAM-Bzp** is not stable in aqueous solution. Thus, after addition of **CGAM-Bzp** in DMEM, the solution should be utilized for the labeling immediately.
3. Incubate the cells at 37°C under 5% CO_2 for 3 h.
4. After removal of the medium, wash the cells twice with serum-free DMEM.
5. Place the dish onto the stage of a CLSM (e.g., Olympus FLUOVIEW FV1000) equipped with an oil immersion objective (60×, NA = 1.40), autofocus device (Z-drift compensation, ZDC), and a GaAsP detector.
6. Acquire fluorescence images using the 488 nm excitation derived from an Ar ion laser for OG, and 543 nm excitation derived from a HeNe laser for mCherry.

4.2 Confirmation of Covalent Labeling to $GABA_AR$ by Western Blotting Analysis

Chemical labeling to target proteins is quantitatively analyzed by Western blotting using antibody specific to a labeled fluorophore. In this method, the labeled proteins are analyzed on the basis of molecular weight after denaturation with SDS, which gives us direct information about covalent labeling of the fluorophore to target proteins. In addition, the selectivity of chemical labeling to target proteins can be quantitatively confirmed by comparing the band intensity.

We checked selective labeling by detecting the band corresponding to the molecular weight of $GABA_ARs$ using **CGAM-Gaba**, **CGAM-Bzp**, or **CGAM-Bbr** in cells transfected with α1/β3/γ2 $GABA_ARs$ (Fig. 6). The labeled band was not observed in empty vector-transfected cells or α1/β3/γ2 $GABA_AR$-transfected cells pretreated with the competitive inhibitor, indicating good selectivity of the chemical labeling to $GABA_ARs$. Although $GABA_ARs$ form a heteropentamer consisting of α1-, β3-, and γ2-subunits, we can estimate labeled subunits from the molecular weight difference of the labeled band (Fig. 6B). The protocol is described later.

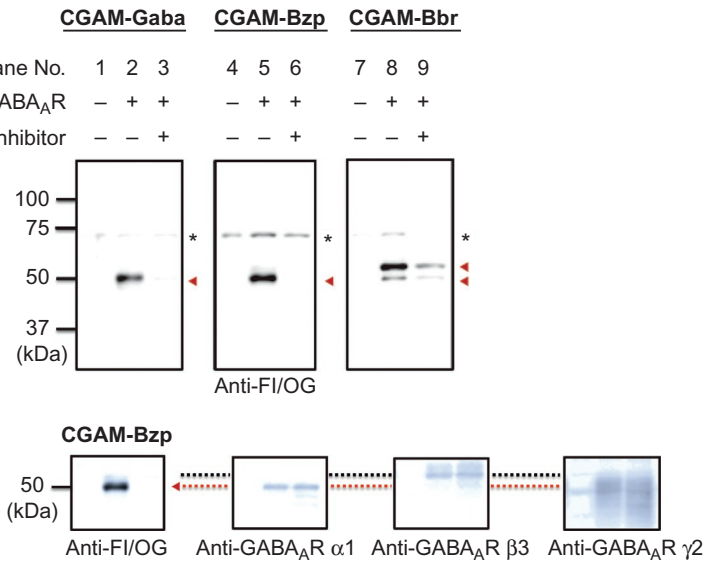

Fig. 6 Chemical labeling of $GABA_AR$s in HEK293T cells using CGAM reagents. (A) For GABA-site labeling, HEK293T cells transfected with α1/β3/γ2 $GABA_AR$s ($GABA_AR(+)$) or the control vector ($GABA_AR(-)$) were treated with 1 μ*M* CGAM-Gaba in the presence or absence of 20 μ*M* gabazine. For benzodiazepine-site labeling, the cells were treated with 1 μ*M* CGAM-Bzp in the presence or absence of 20 μ*M* flumazenil. For barbiturate-site labeling, the cells were treated with 10 μ*M* CGAM-Bbr in the presence or absence of 1 m*M* amobarbital. These reactions are conducted in serum-free DMEM at 37°C for 1 h. *Red arrowhead* indicates labeled $GABA_AR$s. * indicates nonspecific labeling of bovine serum albumin (BSA) included in the culture medium. (B) Comparison of the molecular weight between labeled band detected by anti-Fl/OG antibody and $GABA_AR$ subunits detected by anti-$GABA_A$ α1, anti-$GABA_A$ β3, or anti-$GABA_A$ γ2 antibody. *Reproduced from Yamaura, K., Kiyonaka, S., Numata, T., Inoue, R., & Hamachi, I. (2016). Discovery of allosteric modulators for $GABA_A$ receptors by ligand-directed chemistry.* Nature Chemical Biology, 12, *822–830, with permission from Nature Publishing Group.*

1. After 42–54 h of transfection in 3.5 cm dishes, replace the culture medium with serum-free DMEM containing LDAI reagent.
2. Incubate the cells at 37°C under 5% CO_2 for 3–4 h.
3. Remove the medium containing LDAI reagent.
4. Add 1 mL PBS and dissociate labeled cells from the dishes by pipetting.
5. Transfer the suspension to microcentrifuge tubes and centrifuge ($600 \times g$, 2 min, 4°C).
6. Remove PBS and wash the cells twice with PBS.
7. Lyse the cells with 50 μL RIPA (25 m*M* Tris/HCl, 150 m*M* NaCl, 1% NP-40, 0.25% deoxycholate (DOC), 0.1% SDS, pH 7.4) buffer

containing protease inhibitor (Calbiochem, 39134) and rotate at 4°C for 30 min.

8. Centrifuge (10,000 × *g*, 10 min, 4°C) and collect the supernatant.
9. Mix the lysate with 5 × SDS-PAGE loading buffer (325 m*M* Tris–HCl, 15% SDS, 20% sucrose, 0.5 *M* DTT, and 0.02% BPB, pH 6.8) and incubate for 1 h at room temperature.
10. Apply to SDS-PAGE and electrotransfer onto immune-blot PVDF membranes (Bio-rad).
11. Block the membrane with 5% nonfat dry milk in TBS containing 0.05% Tween 20 (Sigma-Aldrich).
12. Stain these membranes with rabbit antifluorescein/Oregon Green antibody (Abcam, ab19491, ×2000), rabbit anti-$GABA_AR$ α1 antibody (Millipore, 06-868, ×1000), rabbit anti-$GABA_AR$ β3 antibody (Rockland, 600-401-C79, ×1000), rabbit anti-$GABA_AR$ γ2 antibody (Rockland, 612-401-C81, ×1000).
13. Stain these membranes with an HRP-conjugated goat antirabbit IgG (Santa Cruz, SC-2004, ×5000).
14. Develop these membranes with ECL Prime Western blotting detection system (GE Healthcare) and analyze with a fluorescent imaging system (LAS4000, GE Healthcare).

4.3 Determination of Labeling Yield to $GABA_ARs$ Using Fluorophore-Conjugated Ligand by CLSM

The labeling yield of **CGAM-Bzp** to $GABA_ARs$ on the cell surface can be determined by CLSM imaging under live cell conditions. Here, we utilized OG-conjugated flurazepam (**Bzp-OG**) (Fig. 7A). After incubation of **Bzp-OG** in the cells transfected with α1/β3/γ2 $GABA_ARs$, CLSM visualized the prominent fluorescence from the cell surface, by which intensity we can estimate surface-expressed $GABA_ARs$. On the assumption that the fluorescent properties of **Bzp-OG** noncovalently bound to $GABA_ARs$ are similar to that of OG labeled to $GABA_ARs$ covalently by **CGAM-Bzp**, we can evaluate the labeling yield by comparing the fluorescence intensity in the presence or absence of **Bzp-OG** in the labeled cells (Fig. 7B). Although this method is useful, significant background fluorescence was observed in some cases due to the excess of **Bzp-OG** in the medium, which may seriously interfere with the precise evaluation. To ignore the background fluorescence, we concurrently analyze the fluorescence intensity obtained from

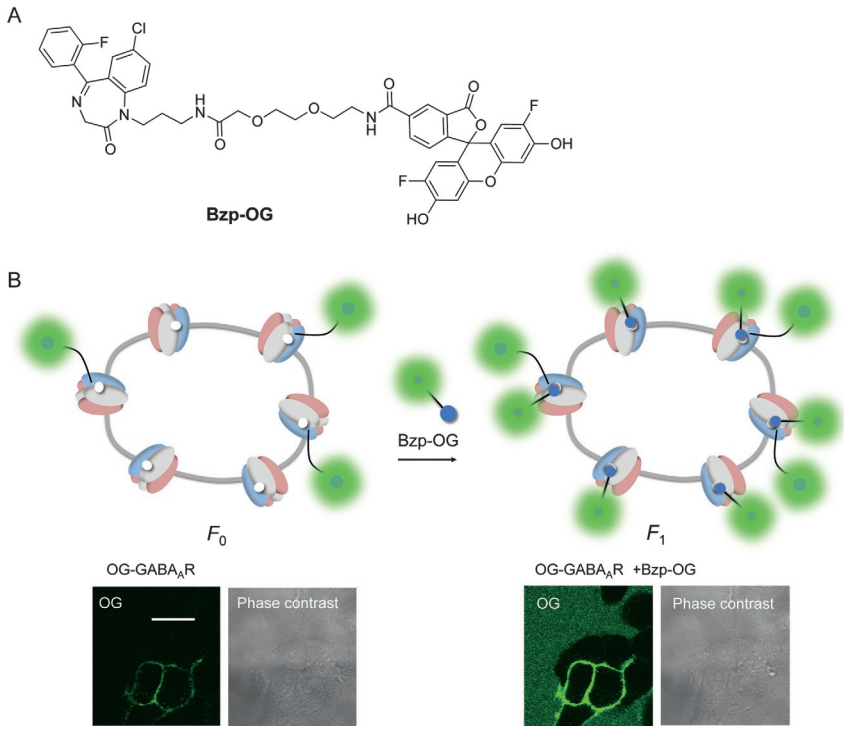

Fig. 7 Determination of the labeling yield for benzodiazepine site on GABA$_A$Rs labeled by CGAM-Bzp. (A) Chemical structure of Bzp-OG. (B) Determination of the labeling yield for OG-labeled GABA$_A$Rs using Bzp-OG. Schematic illustration of the fluorescent changes (*upper*) and representative confocal images (*lower*) are shown. Scale bars: 20 μm. *Reproduced from Yamaura, K., Kiyonaka, S., Numata, T., Inoue, R., & Hamachi, I. (2016). Discovery of allosteric modulators for GABA$_A$ receptors by ligand-directed chemistry.* Nature Chemical Biology, *12, 822–830, with permission from Nature Publishing Group.*

the intercellular interface in CLSM imaging. The detailed protocols were described as follows.

1. Obtain confocal image of labeled GABA$_A$Rs (F_0) as described in Section 4.1.
2. Add 0.1 μ*M* **Bzp-OG**. *Note*: fluorescent titration experiments by CLSM have revealed that **Bzp-OG** binds to most of GABA$_A$Rs on cell surface in this condition (data not shown).
3. After 1 min, obtain confocal image of labeled GABA$_A$Rs (F_1).
4. Quantitatively measure fluorescence intensity from plasma membrane of single labeled cell using the Fluoview software (Olympus).

5. Determine the labeling yield for benzodiazepine site on $GABA_A$Rs based on the following equation: $\text{labeling yield} = F_0/(F_1 - F_0) \times 100$.

4.4 Identification of Labeling Site for Drug Binding Site by Peptide Mass Fingerprinting Analysis

The labeling site of $GABA_A$Rs by **CGAM-Bzp** was determined using peptide mass fingerprinting analysis (Fig. 8). To enrich the OG-labeled $GABA_A$Rs, the labeled cell lysate was immunoprecipitated using OG-specific antibody. Then, the immunoprecipitate fraction was separated by SDS-PAGE, and the OG-labeled band was excised using a fluorescent gel imager. After in-gel digestion with trypsin, the peptides were analyzed by LC-MS/MS analysis. The obtained data were further analyzed using Proteome Discoverer and SEQUEST programs to determine the labeled site. The detailed protocols are described later.

1. Collect the supernatant of the cell lysate after labeling (for details, see step 8 in Section 4.2).
2. Add anti-Fl/OG antibody (ab19491, ×400) to the cell lysate and rotate at 4°C for 18 h.
3. Add Dynabeads® Protein A (Thermo Fisher Scientific) to a different tube and wash the beads with RIPA buffer.
4. Add the lysate treated with antibody to the tube containing Dynabeads® Protein A and rotate at 4°C for 2 h.
5. Wash the beads three times with RIPA buffer.
6. Add 2× SDS-PAGE sample buffer (125 m*M* Tris–HCl, 4% SDS, 20% glycerol, 0.01% bromophenol blue, pH 6.8) and boil in heat block for 5 min.
7. Collect the supernatant and apply to SDS-PAGE.
8. Excise the labeled band corresponding to $GABA_A$R using fluorescence gel imager (LAS4000, GE Healthcare).
9. Perform in-gel digestion using MS grade Trypsin (Thermo Fisher Scientific).
10. Analyze the peptide by nanoflow reverse phase liquid chromatography followed by tandem MS, using a LTQ Orbitrap XL hybrid mass spectrometer (Thermo Fisher Scientific).
11. Record peptide spectra using Xcalibur 2.1 system (Thermo Fisher Scientific)
12. Analyze the peptide spectra by Proteome Discoverer 1.4.1.14 (Thermo Fisher Scientific).

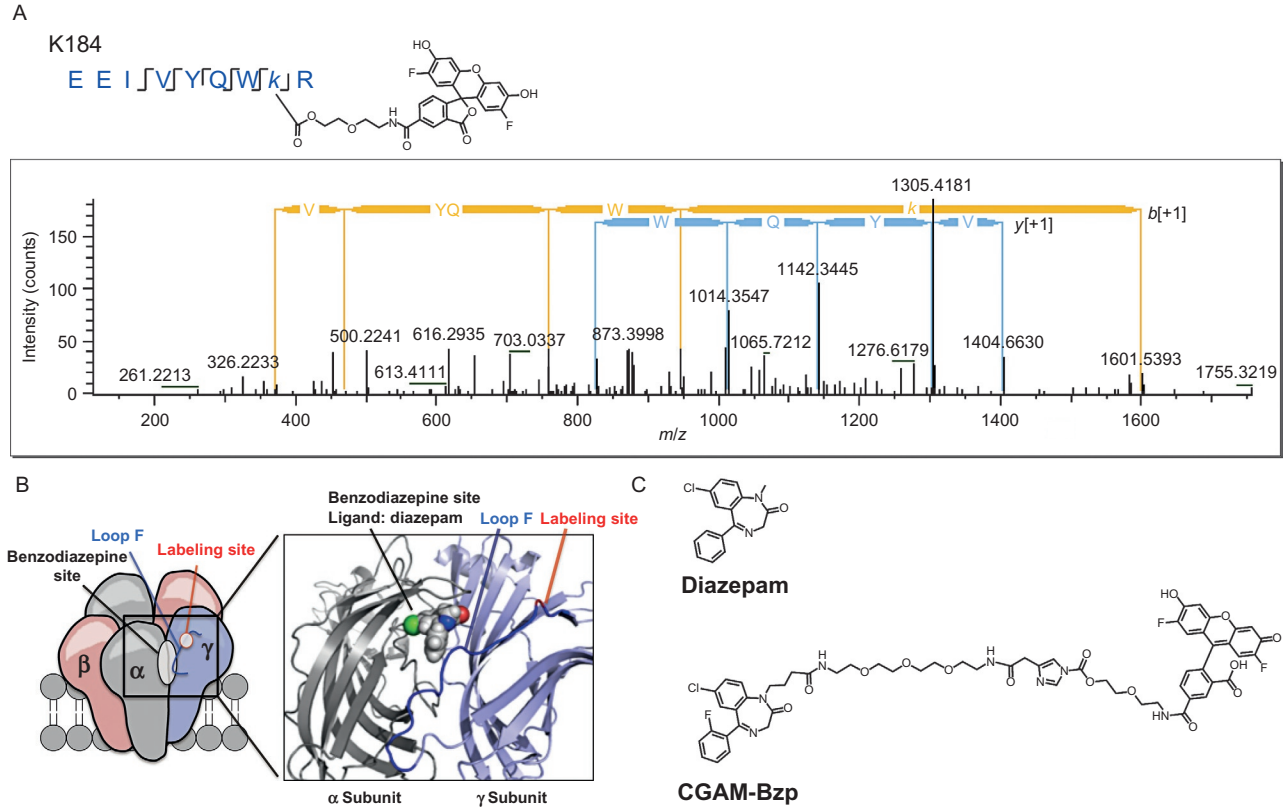

Fig. 8 See legend on next page.

13. Perform the analysis using the SEQUEST HT (Thermo Fisher Scientific) against latest uniprot database for $GABA_AR$ α1 subunit (GBRA1_MOUSE, P62812), $GABA_AR$ β3 subunit (GBRB3_MOUSE, P63080), and $GABA_AR$ γ2 subunit (GBRG2_MOUSE, P22723).

5. CONSTRUCTION OF FLUORESCENT BIOSENSORS USING LABELED $GABA_ARs$

As described in Section 1, we have developed fluorescent biosensors capable of detecting competing ligands using chemical labeling coupled with the BFQR system (Fig. 1, Wang et al., 2011). In this method, molecular design of the quencher–ligand conjugate is crucial for best sensitivity. Thus, we first discuss our design strategy of the quencher–ligand conjugate and subsequently describe how to construct the fluorescent biosensor for $GABA_AR$ ligands using BFQR system in this section.

5.1 Molecular Design of Quencher–Ligand Conjugates for $GABA_ARs$

Quencher–ligand conjugates consist of three modules: (a) a fluorescence quencher moiety, (b) a ligand moiety having affinity to the target protein, (c) a spacer between quencher and the ligand. For $GABA_ARs$, we developed two types of quencher–ligand conjugates (**Gaba-Q** or **Bzp-Q**) binding to the orthosteric GABA site or allosteric benzodiazepine site, respectively (Fig. 9) (Yamaura et al., 2016). Here, we describe the molecular design of the quencher–ligand conjugate for the benzodiazepine site (**Bzp-Q**) as follows.

1. A suitable chemical structure of the quencher moiety is the most crucial for sufficient fluorescence quenching of the labeled fluorophore. In our

Fig. 8 Identification of labeled site for benzodiazepine binding site on $GABA_ARs$ using CGAM-Bzp by peptide mass fingerprinting analysis. (A) MS/MS analysis of the OG-modified peptide detected from γ2 subunit of OG-labeled $GABA_ARs$. (B) Structural illustration and structure model based on homology models and docking studies of $GABA_AR$ (nchembio.917-s2.pdb). Loop F and the amino acid modified by CGAM-Bzp are shown as *blue* and *red* in the cartoon, respectively. Hydrogen, nitrogen, oxygen, and chlorine atom of diazepam ligand are shown as *gray*, *blue*, *red*, and *green spheres*, respectively. (C) Chemical structure of diazepam and CGAM-Bzp. *Reproduced from Yamaura, K., Kiyonaka, S., Numata, T., Inoue, R., & Hamachi, I. (2016). Discovery of allosteric modulators for $GABA_A$ receptors by ligand-directed chemistry.* Nature Chemical Biology, 12, *822–830, with permission from Nature Publishing Group.*

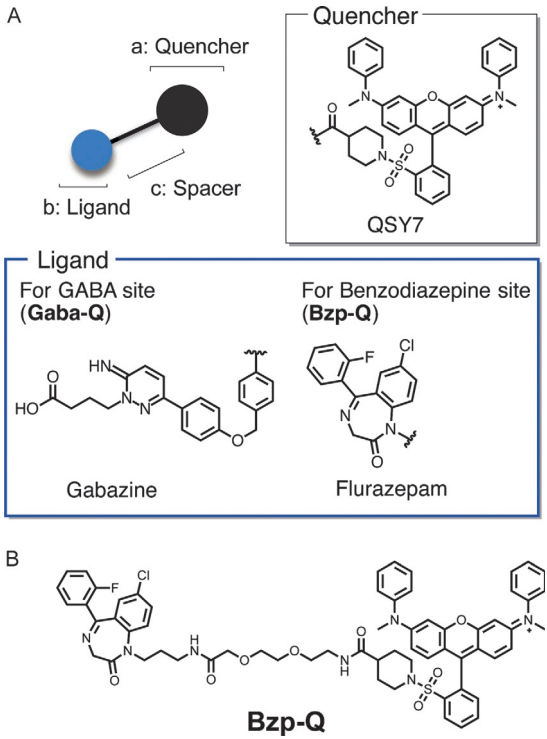

Fig. 9 Molecular design of quencher–ligand conjugates for $GABA_ARs$. (A) Basic design configuration of quencher–ligand conjugates for $GABA_ARs$. (B) Chemical structure of quencher–ligand conjugate (Bzp-Q) for benzodiazepine site of $GABA_ARs$.

BFQR system, the quenching relies on FRET between the fluorescent label and the bound quencher. Thus, the absorption spectrum of the acceptor (quencher) molecule should overlap well with the emission spectrum of the donor (fluorophore) molecule for efficient quenching. In this case, we chose QSY7 as a quencher moiety, exhibiting a high quenching efficiency for labeled OG thanks to the substantial overlap of these spectra (Wruss et al., 2009).

2. The spacer moiety of quencher–ligand conjugate is also important for the fluorescence quenching because FRET is strongly dependent on the distance and relative orientation between the donor (fluorophore) and acceptor (quencher) molecules. In our example, we prepared quencher–ligand conjugates having different spacer lengths for the benzodiazepine site on $GABA_ARs$ (unpublished results); one of the optimized structures is **Bzp-Q** as shown in Fig. 9B.

5.2 Construction of Fluorescent Biosensor for $GABA_ARs$ Employing the BFQR System

A schematic illustration of BFQR system on $GABA_ARs$ is shown in Fig. 10A. The fluorescence intensity following LDAI labeling, where the fluorophore is covalently attached in the vicinity of the ligand-binding site, is defined as F_0. The labeled fluorescence can then be efficiently quenched upon the juxtaposition of a quencher by addition of the quencher–ligand conjugate, and the fluorescence intensity in this step is defined as F_1. When small molecules having a sufficient affinity to the binding site identical with that of the ligand–quencher conjugate are added to the culture medium, the quencher–ligand conjugate bound to the ligand-binding site is competitively released, which results in the fluorescence recovery (F_2). This system can provide the "turn-on" type of fluorescent biosensor (Fig. 10A and B). Using this strategy, we developed two fluorescent sensors, each of which can respond to orthosteric GABA-site ligands or allosteric benzodiazepine-site ligands for $GABA_ARs$ (Yamaura et al., 2016). Importantly, these biosensors discriminated between the target-site ligands and those designed to interact with other sites (Fig. 10C). Moreover, we can quantitatively determine the ligand affinity by the concentration-dependent change of the fluorescence ratio (F_2/F_1), which is discussed in Section 6. Here, the procedures for construction of a fluorescent biosensor for benzodiazepine are described in detail.

1. Label $GABA_ARs$ using **CGAM-Bzp** on glass-bottom dishes as described in Section 4.1.
2. After removal of the medium, add 100 μL of serum-free DMEM and obtain the confocal images (F_0).
3. Add 100 μL of serum-free DMEM including 2 μ*M* **Bzp-Q** (total volume 200 μL) and incubate for 1 min.
4. Obtain the confocal image (F_1).
5. Add 200 μL of serum-free DMEM including the ligand (e.g., 2 μ*M* flumazenil) and 1 μ*M***Bzp-Q** (total volume 400 μL) and incubate for 1 min.
6. Obtain the confocal image (F_2).
7. Using imageJ software (NIH), subtract the background fluorescence in all images.
8. Measure fluorescence intensity (F_0, F_1, and F_2) from plasma membrane in single cells in these images using imageJ software.
9. *Caution*: The DMSO stock of quencher–ligand conjugates should be stored in the freezer. After diluting the stock solution with serum-free DMEM, immediately utilize for experiment to prevent aggregation in the solution or adsorption to the microtube.

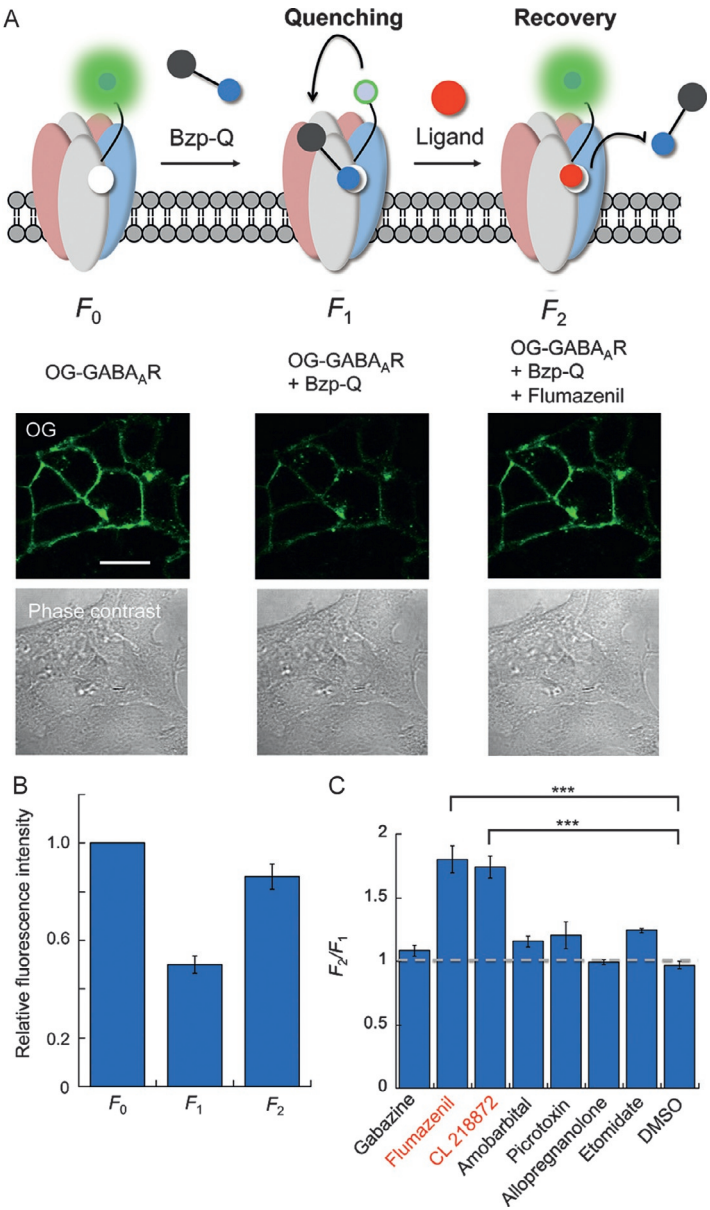

Fig. 10 Construction of GABA$_A$R-based biosensors for benzodiazepine ligands by BFQR system. (A) Fluorescence quenching of OG-labeled GABA$_A$R by 1 μ*M* Bzp-Q and the recovery following addition of 200 μ*M* flumazenil. Schematic illustration (*upper*) and representative confocal images (*lower*) are shown. HEK293T cells transfected with α1/β3/γ2 GABA$_A$Rs were labeled by 2 μ*M* CGAM-Bzp(OG-GABA$_A$R). Scale bars: 20 μm. (B) Relative intensity of labeled (F_0), quenched (F_1), and recovered fluorescence (F_2).

Caution in the fluorescent assay: This BFQR method is powerful for detecting ligands which competitively bind to the quencher–ligand conjugate. However, it was found that these sensors can detect not only competitive ligands but also noncompetitive ligands, which induce structural changes of the receptor upon the ligand binding in some cases (Yamaura et al., 2016). Therefore, the competitive radioligand binding assay should be considered for confirming whether these ligands bind to the receptors competitively or noncompetitively.

6. QUANTITATIVE ANALYSIS OF LIGAND AFFINITY USING BFQR-BASED BIOSENSORS

In this section, we describe quantitative analysis of the ligand affinity on $GABA_ARs$ using the BFQR system. The "turn-on" type fluorescent sensors usually show concentration-dependent fluorescent changes after addition of the corresponding $GABA_ARs$ ligands, and the apparent binding constants (K_{app}) can be determined from the titration (saturation) curve. When the ligand competitively binds to the quencher–ligand conjugate, the real affinity (the K_d value) of the ligand to $GABA_ARs$ can be calculated using the K_{app} of the ligand and the K_a value of the quencher–ligand conjugate (($K_{a(quencher)}$) value). The detailed protocols for the determination of the K_d values of benzodiazepine-site ligands are described as follows; the K_d values of GABA-site ligands can be determined by similar procedures.

6.1 K_d Determination of Bzp-Q

To calculate K_d values of competitive ligands in our BFQR method, we need the $K_{a(quencher)}$ value of the quencher–ligand conjugate. The procedures for **Bzp-Q** are described as follows (Fig. 11).

1. Label $GABA_ARs$ using **CGAM-Bzp** on glass-bottom dishes as described in Section 4.1.

Fig. 10—Cont'd The fluorescence intensity was obtained from confocal imaging, $n = 3$. (C) Specificity of the fluorescent biosensor for $GABA_AR$ ligands. The F_2/F_1 ratio after addition of each ligand is shown. Each ligand concentration is the following: gabazine (1 m*M*), flumazenil (10 μ*M*), CL217782 (0.05 m*M*), amobarbital (1 m*M*), picrotoxin (1 m*M*), allopregnanolone (0.05 m*M*), and etomidate (1 m*M*), $n = 3$. $^{***}P < 0.001$. Data represent mean ± SEM. *Reproduced from Yamaura, K., Kiyonaka, S., Numata, T., Inoue, R., & Hamachi, I. (2016). Discovery of allosteric modulators for $GABA_A$ receptors by ligand-directed chemistry.* Nature Chemical Biology, 12, *822–830, with permission from Nature Publishing Group.*

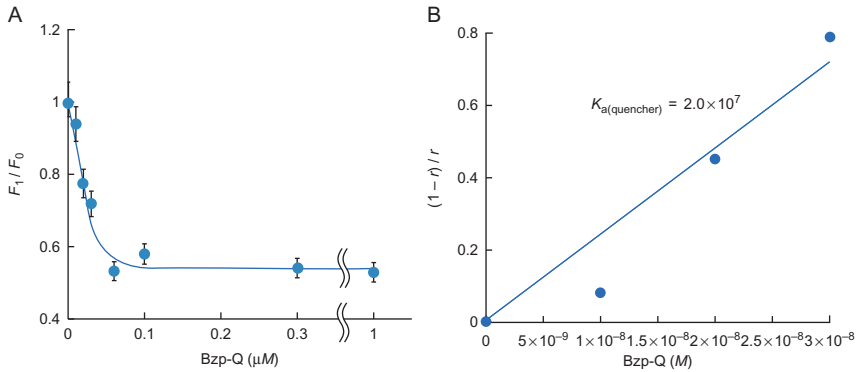

Fig. 11 K_d determination for Bzp-Q. (A) Concentration-dependency of Bzp-Q for the F_1/F_0 ratio of OG-GABA$_A$R, $n = 3$. Data represent mean ± SEM. (B) The values determined from the fluorescence titration curve (A) can be plotted to obtain a linear curve with slope. The K_d value (50 n*M*) was directly calculated from the curve by the Hill plot. *Reproduced from Yamaura, K., Kiyonaka, S., Numata, T., Inoue, R., & Hamachi, I. (2016). Discovery of allosteric modulators for GABA$_A$ receptors by ligand-directed chemistry.* Nature Chemical Biology, 12*, 822–830, with permission from Nature Publishing Group.*

2. After removal of the medium, add 100 μL of serum-free DMEM and obtain the confocal images (F_0).
3. Add 100 μL of serum-free DMEM including each concentration of **Bzp-Q** (total volume 200 μL) and incubate for 1 min.
4. Obtain the confocal image (F_1) at each concentration of **Bzp-Q**.
5. Using the imageJ software, subtract the background fluorescence in all images.
6. Determine K_d value of **Bzp-Q** by the Hill plot using the following equation.

$$(1-r)/r = K_{a(quencher)} \times [quencher]$$
$$K_{d(quencher)} = 1/K_{a(quencher)}$$
r : relative fluorescence intensity

Note: F_0 and saturated F_1 value are defined as 1 and 0, respectively.

6.2 K_d Determination of Competitive Ligands on Benzodiazepine Site

K_{app} of the each ligand for benzodiazepine site was evaluated by fluorescence titration assay, in which the fluorescence intensity on the cell surfaces was measured upon addition of each concentration of the ligand. The real K_d

value for the ligand was determined using K_{app} of the ligand and $K_{a(quencher)}$ of **Bzp-Q**. As a typical example, procedures for determining the K_d value of flumazenil, a typical benzodiazepine-site ligand, are described as follows (Fig. 12).

1. Label $GABA_AR$s using **CGAM-Bzp** on glass-bottom dishes as described in Section 4.1.
2. After removal of the medium, add 100 μL of serum-free DMEM and obtain confocal images (F_0).
3. Add 100 μL of serum-free DMEM including 2 μ*M* **Bzp-Q** (total volume 200 μL) and incubate for 1 min.
4. Obtain the confocal image (F_1).
5. Add 200 μL of serum-free DMEM including each concentration of flumazenil and 1 μ*M* **Bzp-Q** (total volume 400 μL) and incubate for 1 min.
6. Obtain the confocal image (F_2) at each concentration of flumazenil.
7. Using the imageJ software, subtract the background fluorescence in all images.
8. To calculate the apparent association constant for flumazenil ($K_{app(ligand)}$), adapt these values to the following equation.

$$r/(1-r) = K_{app} \times [\text{ligand}]$$
r : relative fluorescence intensity

Note: F_0 and saturated F_2 values were defined as 0 and 1, respectively.

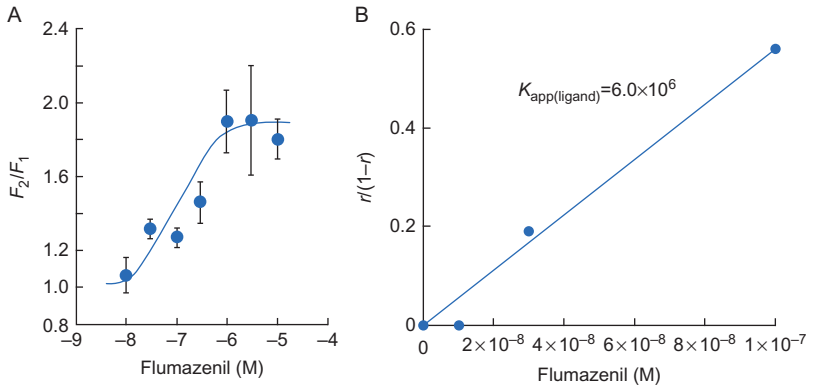

Fig. 12 K_d determination for flumazenil. (A) Concentration-dependency of flumazenil for the F_2/F_1 ratio of OG-$GABA_AR$, $n = 3$. Data represent mean ± SEM. (B) The values determined from the fluorescent titration curve (A) can be plotted to obtain a linear curve with slope. The K_{app} value (6.0×10^6 M^{-1}) was calculated from the curve by the Hill plot, which is utilized for calculation of K_d value of flumazenil.

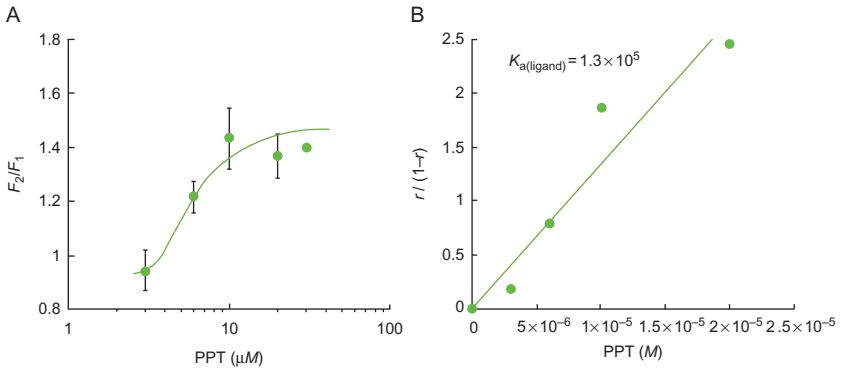

Fig. 13 K_d determination for PPT. (A) Concentration-dependency of PPT for the F_2/F_1 ratio of OG-GABA$_A$R, $n = 3$. Data represent mean ± SEM. (B) The values determined from the fluorescent titration curve (A) can be plotted to obtain a linear curve with slope. The K_d value (7.3 μ*M*) was directly calculated from the curve by the Hill plot.

9. To calculate the real K_d value for flumazenil ($K_{d(ligand)}$), adapt calculated K_{app} value and calculated $K_{a(quencher)}$ value to the following equation

$$K_{a(ligand)} = K_{app(ligand)} + \left(K_{app(ligand)} \times K_{a(quencher)} \times [quencher]\right)$$
$$K_{d(ligand)} = 1/K_{a(ligand)}$$

Caution in calculating the K_d value: In addition to such competitive ligands, it should be noted that our BFQR-based sensors detect noncompetitive ligands which induce structural changes of the receptor upon the ligand binding in some case. In this case, we can directly determine the K_d value of the noncompetitive ligands from the fluorescent titration assay. As a typical example, procedures for determining the K_d value of PPT, a noncompetitive benzodiazepine-site ligand, are shown in Fig. 13.

7. SUMMARY AND FUTURE DIRECTIONS

We describe a strategy and protocols for constructing "turn-on" type fluorescent biosensors based on the GABA$_A$Rs scaffold by coupling ligand-directed chemistry with the BFQR fluorescent readout system. It has been demonstrated that our methods allow for quantitative analysis of ligand affinity for GABA$_A$Rs on the live cell surface. Importantly, we can selectively label structurally complicated membrane receptors with fluorophores without any structural information by ligand-directed chemistry. Thus, our

biosensor system may be extended to various types of membrane-receptors on live cells, if appropriate small molecule ligands are known.

Recently, protein-based biosensors have been recognized as powerful platforms for high-throughput screening (HTS) of drug candidates. As a successful result, Rauh's group reported a HTS for kinase inhibitors using fluorophore-kinase conjugates, termed FLiK assay that is mostly conducted in the purified test tube system (Simard, Pawar, et al., 2009). It has been demonstrated that our BFQR-based biosensors for $GABA_AR$ ligands are highly amenable to the HTS of a chemical library (Yamaura et al., 2016), which can be conducted with live cell systems. We indeed discovered new small molecules acting as negative allosteric modulators for $GABA_ARs$ by this screening. It is widely recognized that the myriad cell-surface receptors represent the largest family of drug targets. Hence, ongoing drug discovery programs may be accelerated by using our biosensor systems in the near future.

ACKNOWLEDGMENTS

This work was funded by the Japan Science and Technology Agency (JST) Core Research for Evolutional Science and Technology (CREST) of Molecular Technologies to I.H. and by SUNBOR Grant from Suntory Foundation for Life Sciences to S.K.

REFERENCES

Barnard, E. A., Skolnick, P., Olsen, R. W., Mohler, H., Sieghart, W., Biggio, G., et al. (1998). International Union of Pharmacology. XV. Subtypes of γ-aminobutyric acidA receptors: Classification on the basis of subunit structure and receptor function. *Pharmacological Reviews*, *50*, 291–314.

Brun, M. A., Tan, K. T., Griss, R., Kielkowska, A., Reymond, L., & Johnsson, K. (2012). A semisynthetic fluorescent sensor protein for glutamate. *Journal of the American Chemical Society*, *134*, 7676–7678.

Brun, M. A., Tan, K. T., Nakata, E., Hinner, M. J., & Johnsson, K. (2009). Semisynthetic fluorescent sensor proteins based on self-labeling protein tags. *Journal of the American Chemical Society*, *131*, 5873–5884.

Chebib, M., & Johnston, G. A. (2000). GABA-activated ligand gated ion channels: Medicinal chemistry and molecular biology. *Journal of Medicinal Chemistry*, *43*, 1427–1447.

Chen, C., Ke, J., Zhou, X. E., Yi, W., Brunzelle, J. S., Li, J., et al. (2013). Structural basis for molecular recognition of folic acid by folate receptors. *Nature*, *500*, 486–489.

Fehr, M., Frommer, W. B., & Lalonde, S. (2002). Visualization of maltose uptake in living yeast cells by fluorescent nanosensors. *Proceedings of the National Academy of Sciences*, *99*, 9846–9851.

Fujishima, S. H., Yasui, R., Miki, T., Ojida, A., & Hamachi, I. (2012). Ligand-directed acyl imidazole chemistry for labeling of membrane-bound proteins on live cells. *Journal of the American Chemical Society*, *134*, 3961–3964.

Hanson, S. M., & Czajkowski, C. (2008). Structural mechanisms underlying benzodiazepine modulation of the $GABA_A$ receptor. *The Journal of Neuroscience*, *28*, 3490–3499.

Loving, G. S., Sainlos, M., & Imperiali, B. (2010). Monitoring protein interactions and dynamics with solvatochromic fluorophores. *Trends in Biotechnology*, *28*, 73–83.

Marvin, J. S., Borghuis, B. G., Tian, L., Cichon, J., Harnett, M. T., Akerboom, J., et al. (2013). An optimized fluorescent probe for visualizing glutamate neurotransmission. *Nature Methods*, *10*, 162–170.

Marvin, J. S., & Hellinga, H. W. (1998). Engineering biosensors by introducing fluorescent allosteric signal transducers: Construction of a novel glucose sensor. *Journal of the American Chemical Society*, *120*, 7–11.

Masharina, A., Reymond, L., Maurel, D., Umezawa, K., & Johnsson, K. (2012). A fluorescent sensor for GABA and synthetic GABAB receptor ligands. *Journal of the American Chemical Society*, *134*, 19026–19034.

Matsuo, K., Kioi, Y., Yasui, R., Takaoka, Y., Miki, T., Fujishima, S. H., et al. (2013). One-step construction of caged carbonic anhydrase I using a ligand-directed acyl imidazole-based protein labeling method. *Chemical Science*, *4*, 2573–2580.

Mayr, L. M., & Bojanic, D. (2009). Novel trends in high-throughput screening. *Current Opinion in Pharmacology*, *9*, 580–588.

Miki, T., Awa, M., Nishikawa, Y., Kiyonaka, S., Wakabayashi, M., Ishihama, Y., et al. (2016). A conditional proteomics approach to identify proteins involved in zinc homeostasis. *Nature Methods*, *13*, 931–937.

Miki, T., Fujishima, S. H., Komatsu, K., Kuwata, K., Kiyonaka, S., & Hamachi, I. (2014). LDAI-based chemical labeling of intact membrane proteins and its pulse-chase analysis under live cell conditions. *Chemistry & Biology*, *21*, 1013–1022.

Morii, T., Sugimoto, K., Makino, K., Otsuka, M., Imoto, K., & Mori, Y. (2002). A new fluorescent biosensor for inositol trisphosphate. *Journal of the American Chemical Society*, *124*, 1138–1139.

Okumoto, S., Looger, L. L., Micheva, K. D., Reimer, R. J., Smith, S. J., & Frommer, W. B. (2005). Detection of glutamate release from neurons by genetically encoded surface-displayed FRET nanosensors. *Proceedings of the National Academy of Sciences of the United States of America*, *102*, 8740–8745.

Olsen, R. W., & Sieghart, W. (2009). $GABA_A$ receptors: Subtypes provide diversity of function and pharmacology. *Neuropharmacology*, *56*, 141–148.

Prével, C., Pellerano, M., Van, T. N. N., & Morris, M. C. (2014). Fluorescent biosensors for high throughput screening of protein kinase inhibitors. *Biotechnology Journal*, *9*, 253–265.

Rudolph, U., & Knoflach, F. (2011). Beyond classical benzodiazepines: Novel therapeutic potential of $GABA_A$ receptor subtypes. *Nature Reviews. Drug Discovery*, *10*, 685–697.

Sieghart, W. (2015). Allosteric modulation of $GABA_A$ receptors via multiple drug-binding sites. *Advances in Pharmacology*, *72*, 53–96.

Simard, J. R., Getlik, M., Grütter, C., Pawar, V., Wulfert, S., Rabiller, M., et al. (2009). Development of a fluorescent-tagged kinase assay system for the detection and characterization of allosteric kinase inhibitors. *Journal of the American Chemical Society*, *131*, 13286–13296.

Simard, J. R., Klüter, S., Grütter, C., Getlik, M., Rabiller, M., Rode, H. B., et al. (2009). A new screening assay for allosteric inhibitors of cSrc. *Nature Chemical Biology*, *5*, 394–396.

Simard, J. R., Pawar, V., Aust, B., Wolf, A., Rabiller, M., Wulfert, S., et al. (2009). High-throughput screening to identify inhibitors which stabilize inactive kinase conformations in p38α. *Journal of the American Chemical Society*, *131*, 18478–18488.

Takaoka, Y., Nishikawa, Y., Hashimoto, Y., Sasaki, K., & Hamachi, I. (2015). Ligand-directed dibromophenyl benzoate chemistry for rapid and selective acylation of intracellular natural proteins. *Chemical Science*, *6*, 3217–3224.

Takikawa, K., Asanuma, D., Namiki, S., Sakamoto, H., Ariyoshi, T., Kimpara, N., et al. (2014). High-throughput development of a hybrid-type fluorescent glutamate sensor

for analysis of synaptic transmission. *Angewandte Chemie, International Edition*, *53*, 13439–13443.
Tamura, T., & Hamachi, I. (2014). Recent progress in design of protein-based fluorescent biosensors and their cellular applications. *ACS Chemical Biology*, *9*, 2708–2717.
Tretter, V., Ehya, N., Fuchs, K., & Sieghart, W. (1997). Stoichiometry and assembly of a recombinant $GABA_A$ receptor subtype. *The Journal of Neuroscience*, *17*, 2728–2737.
Tsukiji, S., Miyagawa, M., Takaoka, Y., Tamura, T., & Hamachi, I. (2009). Ligand-directed tosyl chemistry for protein labeling in vivo. *Nature Chemical Biology*, *5*, 341–343.
Wang, H., Koshi, Y., Minato, D., Nonaka, H., Kiyonaka, S., Mori, Y., et al. (2011). Chemical cell-surface receptor engineering using affinity-guided, multivalent organocatalysts. *Journal of the American Chemical Society*, *133*, 12220–12228.
Wruss, J., Pollheimer, P. D., Meindl, I., Reichel, A., Schulze, K., Schöfberger, W., et al. (2009). Conformation of receptor adopted upon interaction with virus revealed by site-specific fluorescence quenchers and FRET analysis. *Journal of the American Chemical Society*, *131*, 5478–5482.
Yamaura, K., Kiyonaka, S., Numata, T., Inoue, R., & Hamachi, I. (2016). Discovery of allosteric modulators for $GABA_A$ receptors by ligand-directed chemistry. *Nature Chemical Biology*, *12*, 822–830.